

# DETERMINATION OF KOZENY CONSTANT BASED ON POROSITY AND PORE TO THROAT SIZE RATIO IN POROUS MEDIUM WITH RECTANGULAR RODS

Turkuler Ozgumus, Moghtada Mobedi\* and Unver Ozkol

Izmir Institute of Technology, Department of Mechanical Engineering, Gulbahce, Urla, Izmir, Turkey

\* *E-Mail: moghtadamobedi@iyte.edu.tr (Corresponding Author)*

**ABSTRACT:** Kozeny-Carman permeability equation is an important relation for the determination of permeability in porous media. In this study, the permeabilities of porous media that contains rectangular rods are determined, numerically. The applicability of Kozeny-Carman equation for the periodic porous media is investigated and the effects of porosity and pore to throat size ratio on Kozeny constant are studied. The continuity and Navier-Stokes equations are solved to determine the velocity and pressure fields in the voids between the rods. Based on the obtained flow field, the permeability values for different porosities from 0.2 to 0.9 and pore to throat size ratio values from 1.63 to 7.46 are computed. Then Kozeny constants for different porous media with various porosity and pore to throat size ratios are obtained and a relationship between Kozeny constant, porosity and pore to throat size ratio is constructed. The study reveals that the pore to throat size ratio is an important geometrical parameter that should be taken into account for deriving a correlation for permeability. The suggestion of a fixed value for Kozeny constant makes the application of Kozeny-Carman permeability equation too narrow for a very specific porous medium. However, it is possible to apply the Kozeny-Carman permeability equation for wide ranges of porous media with different geometrical parameters (various porosity, hydraulic diameter, particle size and aspect ratio) if Kozeny constant is a function of two parameters as porosity and pore to throat size ratios.

**Keywords:** porous media, numerical simulation, permeability, Kozeny constant, Kozeny-Carman equation

## 1. INTRODUCTION

Fluid flow through porous media is widely encountered in natural and industrial problems. To describe the macroscopic fluid velocity through a porous medium, an equation was proposed by Darcy (Darcy, 1856). The so called Darcy's Law establishes a relation between average (macroscopic) velocity and the fluid macroscopic pressure drop through the porous medium. Eq. (1) is the one dimensional form of the Darcy's Law:

$$\langle u \rangle = -\frac{K}{\mu} \left( \frac{d(p)}{dx} \right)^f \quad (1)$$

where  $K$  is an empirical constant called permeability and  $\mu$  is fluid dynamic viscosity. Permeability depends on the micro-structure of the solid phase in the porous media and is independent of the properties of the fluid (Nakayama, 1995). The main parameters which affect the permeability of a porous medium are porosity, pore shape (or particle shape) and the connection of pores with each other. The determination of permeability is very important for simulating flow in a porous medium and it should be a known value prior to a flow analysis

for practical applications, such as flow in a porous finned receiver of a solar parabolic concentrator (Reddy and Satyanarayana, 2008) or simulation of double-diffusive natural convection in a vertical porous annulus (Kalita and Dass, 2011). There are some proposed equations for the determination of the permeability in the literature (Xu and Yu, 2008). One of the most common permeability equations was derived by Kozeny and Carman (Kozeny, 1927; Carman, 1937). The Kozeny-Carman theory and the derivation of Kozeny-Carman permeability equation are summarized in the following paragraphs. The average velocity for a Hagen-Poiseuille flow in a channel with diameter of  $d_i$  can be found as:

$$\langle u \rangle^f = -\frac{1}{32\mu} \frac{d(p)}{dx} d_i^2 \quad (2)$$

By replacing  $\langle u \rangle = \varepsilon \langle u \rangle^f$  and comparing Eqs. (1) and (2), the permeability value for a flow in a channel can be found as  $K = d_i^2 \varepsilon / 32$ . Kozeny considered the medium as a bundle of capillary channels with the same radius. By combining Hagen-Poiseuille velocity equation with Darcy's Law and using tortuosity concept, the following equation for permeability was proposed by

Kozeny (Kozeny, 1927; Kaviani, 1995):

$$K = \frac{\varepsilon d_p^2}{32\tau} \quad (3)$$

where  $\tau$  is tortuosity. Tortuosity can be defined as the ratio of the actual length of flow path in the porous medium to the length of flow path in the absence of porous medium. The permeability equation of Kozeny was modified later by Carman and the so-called Kozeny-Carman equation was introduced to the literature. Kozeny-Carman equation which predicts the permeability reasonably well for the packed bed of spheres is presented as (Carman, 1937, Kaviani, 1995).

$$K = \frac{\varepsilon d_h^2}{16k_K} \quad (4)$$

where  $d_h$  is the pore hydraulic diameter and  $\varepsilon$  is porosity of the porous medium. The pore hydraulic diameter is defined as:

$$d_h = \frac{4\varepsilon}{[A_0(1-\varepsilon)]} \quad (5)$$

where  $A_0$  is the ratio of the fluid-solid interfacial area to the solid volume.

The symbol of  $k_K$  in Eq. (4) is Kozeny constant which includes the effects of flow path (i.e., tortuosity), particle shape and their connections. Eq. (4) can be also written in terms of the particle diameter of the porous media.

Literature review shows that many studies have been performed for the determination of Kozeny constant. Table 1 shows some details of the available literature studies. Type of the studies, considered porous media and Kozeny constant results are displayed in the table. As seen from Table 1, some of the researchers proposed a fixed value for Kozeny constant while some others established a relationship between Kozeny constant and porosity. Most of the researchers preferred to show the relationship between Kozeny constant and porosity (or other parameters) via tables or graphics. Kozeny constant was given as  $4.8 \pm 0.3$  by Carman for packed beds with uniform spheres (Carman, 1937). Ergun (1952) proposed the value of 150 for Blake-Kozeny constant which equals to  $36k_K$  for packed bed of spheres. The Kozeny constant was given as 7.5 for the square cylinders in cross-flow, 9.5 for the cubes and 9 for the circular cylinders in cross-flow by Nakayama et al. (2007). Li and Gu (2005) studied fluid flow through fibrous and granular beds experimentally and proposed the value of 12.81 for Kozeny constant. In the study of Mathavan and Viraraghavan (1992) about peat beds, the value of Kozeny constant was proposed as 3.4. Eidsath et al. (1983) predicted Kozeny constant for various

arrangements of square blocks and cylinders and Kozeny constant was found as 6.3 for in-line arrangement of blocks with porosity of 0.37. Teruel and Rizwan-uddin (2009) studied fluid flow through staggered square cylinders and Kozeny constant value was found as 8.1875 for low porosity range. Vidal et al. (2009) studied the flow through spherical particles and blocks and they found that Kozeny constant varies between 4.9 and 7.1. Koponen et al. (1997) studied a porous medium constructed with randomly placed identical obstacles (square or rectangular particles). Kozeny constant values between 6.5 and 10.4 were found, numerically.

Some researchers preferred to propose relationships for the determination of Kozeny constant. For instance, Kyan et al. (1970) proposed a relation between Kozeny constant and porosity for the low velocity flows in fibrous beds. Happel and Brenner (1986) proposed a relation for the determination of Kozeny constant for parallel flow along the cylinders. Pacella et al. (2011) studied the permeability of hollow fiber bundles for porosities between 0.45 and 0.55, experimentally. A linear relation between Kozeny constant and porosity was proposed for the determination of Blake-Kozeny constant. Davies and Dollimore (1980) studied the flow through a bed of spheres and an equation which relates Kozeny constant with porosity was proposed. Xu and Yu (2008) derived an analytical expression for the determination of permeability in homogeneous porous medium with solid bars.

Furthermore, the change of Kozeny constant with porosity was also investigated by Heijs and Lowe (1995) for a random array of spheres and a clay soil, Gamrat et al. (2008) for 2-D cylinders in inline and staggered arrangements, Karimian and Straatman (2008) for metal foam structure, Liu and Hwang (2012) for fibrous porous media, Plessis and Woudberg (2008) for flow through the blocks, and Drummond and Tahir (1984) for triangular, square and hexagonal arrays of cylinders in parallel flow. Singh and Mohanty (2000), Chen and Papathanasiou (2006) and Bechtold and Ye (2003) studied the effects of inter fiber spacing on Kozeny constant in addition to porosity for fluid flow in fibrous porous media. As can be seen from the above literature review, Kozeny-Carman equation is one of the most encountered permeability equation, however, its application is limited due to the Kozeny constant. As seen from Table 1, the value of Kozeny constant is fixed for a specific porous medium. Some attempts were performed to make a link between Kozeny constant and porosity in order to

Table 1 Literature studies on determination of Kozeny constant.

Researchers	Type of study	Porous medium	Proposed constant or relationship
Xu and Yu (2008)	Theoretical	Cross flow, Inline cylindrical bars	Graphical presentation
Carman (1937)	Experimental	Uniform spheres	$k_K = 4.8 \pm 0.3$
Ergun (1952)	Experimental	Spheres	150 (Blake-Kozeny constant which equals to $36k_K$ for spheres)
Nakayama et al. (2007)	Computational	Square rods, cubes, cylinders	$k_K = 7.5$ for square rods in cross flow $k_K = 9.5$ for cubes $k_K = 9$ for circular cylinders in cross flow
Heijs and Lowe (1995)	Computational	Random spheres and soil sample	Graphical and table presentations
Li and Gu (2005)	Experimental	Fibrous and granular beds	$k_K = 12.81$
Mathavan and Viraraghavan (1992)	Experimental	Peat beds	$k_K = 3.4$
Eidsath et al. (1983)	Computational	Cross flow, In-line blocks, In-line and staggered cylinders	Table presentation
Terual and Rizwan-uddin (2009)	Computational	Cross flow, Staggered square cylinders	$k_K = 8.1875$ for $\varepsilon < 55$
Vidal et al. (2009)	Computational and experimental	Spherical particles and blocks	$4.9 < k_K < 7.1$
Koponen et al. (1997)	Computational	Random porous media constructed with square obstacles	$6.5 < k_K < 10.4$
Singh and Mohanty (2000)	Computational	Generated 3D porous media	Graphical presentation
Chen and Papatthanasiou (2006)	Computational	Disordered fiber arrays	Graphical presentations
Gamrat et al (2008)	Computational	Cross flow, Square rods in inline and staggered arrangements	Graphical presentation
Karimian and Straatman (2008)	Computational	Foam	Graphical presentations
Liu and Hwang (2012)	Computational	Fibrous porous media	Graphical presentations
Plessis and Woudberg (2008)	Computational	Blocks	Graphical and table presentations
Bechtold and Ye (2003)	Computational	Fibres	Graphical presentations
Drummond and Tahir (1984)	Theoretical	Parallel flow for triangular, square and hexagonal arrays of cylinders	Table presentation
Kyan et al. (1970)	Theoretical and experimental	Fibrous beds	$k_K = \frac{\left[ 62.3 \left( \sqrt{\frac{2\pi}{1-\varepsilon}} - 2.5 \right)^2 (1-\varepsilon) + 107.4 \right] \varepsilon^3}{16 \varepsilon^6 (1-\varepsilon)^4}$
Happel and Brenner (1986)	Theoretical	Parallel flow along cylinders, Cross flow through cylinders, Flow through random orientation of spheres, flow through spheres	For parallel flow along cylinders: $k_K = \frac{2\varepsilon^3}{(1-\varepsilon) \left( 2 \ln \left( \frac{1}{1-\varepsilon} \right) - 3 + 4(1-\varepsilon) - (1-\varepsilon)^2 \right)}$ For cross flow through cylinders: $k_K = \frac{2\varepsilon^3}{(1-\varepsilon) \left( \ln \left( \frac{1}{1-\varepsilon} \right) - (1 - (1-\varepsilon)^2) / (1 + (1-\varepsilon)^2) \right)}$ Table presentations
Pacella et. al. (2011)	Experimental	Hollow fibres bundle	$BK = 542\varepsilon - 128$ (Blake-Kozeny constant which equals to $36k_K$ for spheres)
Davies and Dollimore (1970)	Theoretical and experimental	Bed of sedimenting spheres/fluidized beds	$k_K = 1/[2\varepsilon^{n-3}(1-\varepsilon)]$

enhance the application of the Kozeny-Carman equation.

As seen from Eq. (4), Kozeny constant is directly related to tortuosity (Carman, 1937). Different parameters such as porosity, pore to throat size ratio, geometry, size and uniformity of particles (and pores), periodicity and isotropy of porous structure play an important role in the value of tortuosity; however the value of Kozeny constant

is determined based on two parameters as porosity and pore to throat size ratio in this study since the considered porous structure is isotropic, periodic and uniform. There is no doubt that additional microstructural parameters should also be taken into account for complex porous structures.

The aim of the present study is to consider the effects of porosity and pore to throat size ratio

firstly to understand the mechanism of flow in the porous media with rectangular rods and secondly to develop a widely applicable relationship for the determination of Kozeny constant . The study is performed for the square periodic structural units of rectangular rods with different pore to throat size ratios and porosities. The results of study show that the permeability value of two porous media having the same porosity and hydraulic pore diameter may be different from each other. Therefore, the effects of pore to throat size ratio should be involved for the development of a relation for Kozeny constant. A mathematical expression for the determination of Kozeny constant applicable to porous media having different porosity, hydraulic diameter and pore to throat size ratio is suggested. The obtained results are valid for the periodic porous media consisting of rectangular rods with inline arrangement, porosities from 0.2 to 0.9 and pore to throat size ratios values from 1.63 to 7.46.

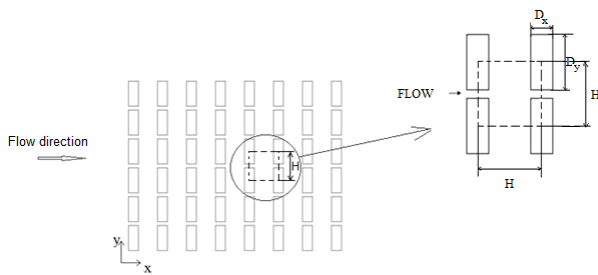


Fig. 1 Schematic view of considered porous media.

**2. CONSIDERED POROUS MEDIA**

The physical model for the considered porous media and the structural unit which is the computational domain are shown in Fig. 1. The porous medium is an infinite medium which consists of rectangular rods. A periodical structural unit with the dimensions of  $H \times H$  ( $1 \times 1 \text{ cm}^2$ ) is chosen as the computational domain. The flow is assumed fully developed and periodical. The length and height of the structural unit is held constant for all studied cases in this paper. The particles (rectangular rods) are placed with in-line arrangement. The rectangular rods have dimensions of  $D_x$  and  $D_y$ . In this study, the pore to throat size ratio is defined as  $\beta = H / (H - D_y)$  and this value is changed from 1.63 to 7.46. The minimum achievable porosities for the considered  $\beta$  values are shown in Table 2. As a sample, the geometrical properties of the studied structural units are given in Table 3 for porous media with porosity of 0.7. The fluid flowing through the medium is assumed to be Newtonian and

incompressible with constant thermophysical properties. The fluid flow is in the laminar regime and the study is performed for the Darcian region ( $Re < 1$ ).

Table 2 Minimum achievable porosities for considered pore to throat size ratios.

$\beta$	Porosity of channel flow
1.63	0.613
2.21	0.452
3.04	0.329
4.44	0.225
7.46	0.134

Table 3 Geometric properties of investigated structural units (for  $\epsilon = 0.7$ ).

	$\beta = 1.63$	$\beta = 2.21$	$\beta = 3.04$	$\beta = 4.44$	$\beta = 7.46$
$A^*$	0.5	1	1.5	2	2.5
$\epsilon$	0.7	0.7	0.7	0.7	0.7
$D_x/H$	0.776	0.547	0.446	0.387	0.346
$D_y/H$	0.388	0.547	0.670	0.774	0.866
$d_p/H$	1.207	1.276	1.250	1.207	1.154
$d_v/H$	0.776	0.820	0.804	0.776	0.742

**3. MICROSCOPIC AND MACROSCOPIC GOVERNING EQUATIONS**

As it was mentioned above, the flow in the voids between the rectangular rods is assumed incompressible and steady. The continuity and momentum equations should be solved in order to determine the velocity and pressure fields in the voids between the rods:

$$\frac{\partial u}{\partial x} + \frac{\partial v}{\partial y} = 0 \tag{6}$$

$$u \frac{\partial u}{\partial x} + v \frac{\partial u}{\partial y} = -\frac{1}{\rho} \frac{\partial p}{\partial x} + \nu \left( \frac{\partial^2 u}{\partial x^2} + \frac{\partial^2 u}{\partial y^2} \right) \tag{7}$$

$$u \frac{\partial v}{\partial x} + v \frac{\partial v}{\partial y} = -\frac{1}{\rho} \frac{\partial p}{\partial y} + \nu \left( \frac{\partial^2 v}{\partial x^2} + \frac{\partial^2 v}{\partial y^2} \right) \tag{8}$$

where  $u$  and  $v$  are the velocity components in  $x$  and  $y$  directions (Fig. 1) and  $p$  is pressure.  $\rho$  and  $\nu$  are density and kinematic viscosity of fluid, respectively. Non-slip boundary condition is applied at the solid surfaces. Boundary conditions are chosen as symmetry for the top and the bottom of the structural unit. At the beginning, a fully developed velocity profile is defined for the fluid inlet boundary. The velocity gradient at the fluid outlet boundary is assumed zero, hence no diffusion transport exists. After solving the governing equations and obtaining the velocity and pressure distributions in the structural unit, the outlet velocity profile is substituted to the inlet boundary. This iterative procedure continues until the same velocity distribution at the inlet and outlet boundaries are obtained. The value of

permeability is also calculated at each iteration step and iterative procedure also continues until no change on the value of permeability is observed. Mathematically, the defined boundary conditions can be presented as:

On the solid walls:

$$u = v = 0 \tag{9}$$

For the top and the bottom boundaries:

$$\frac{\partial u}{\partial y} = \frac{\partial v}{\partial y} = 0 \tag{10}$$

For the inlet boundary:

$$u(0,y) = f(y), v(0,y) = 0 \tag{11}$$

For the outlet boundary:

$$\frac{\partial u}{\partial x}(H,y) = 0 \tag{12}$$

By solving Eqs. (6-8) with the boundary conditions presented above, the velocity and pressure fields inside the pores of the structural units are obtained. In order to obtain the value of permeability, the macroscopic velocity and pressure drop values should be determined. The macroscopic velocity is defined as:

$$\langle u \rangle = \frac{1}{H^2} \int_0^H \int_0^H u dx dy \tag{13}$$

Additionally, the macroscopic pressure gradient value can be defined as (Nakayama et al., 2002):

$$-\frac{d(p)^f}{dx} = \frac{1}{H(H-D_y)} \int_{-(H-D_y)/2}^{(H-D_y)/2} (p|_{x=0} - p|_{x=H}) dy \tag{14}$$

For the studied Reynolds numbers, the Darcy's Law, Eq. (1), is valid and it can be made dimensionless by rearranging the parameters:

$$-\frac{H}{\rho \langle u \rangle^2} \text{Re} \frac{d(p)^f}{dx} = \frac{H^2}{K} \tag{15}$$

where  $\text{Re} = \rho \langle u \rangle H / \mu$ . Eq. (15) is the dimensionless form of Darcy's Law and the term on the left hand side is called as the dimensionless macroscopic pressure drop through the porous medium while  $K/H^2$  is the dimensionless permeability. As can be seen from Eq. (15) there is a linear relationship between the dimensionless pressure drop and the inverse of dimensionless permeability. This relation is only accurate in the Darcian region in which  $\text{Re} < 1$ . Since the permeability only depends on the porous structure and independent of the fluid and flow properties, its value for a structural unit should be a constant. Consequently, the value of dimensionless pressure drop should be identical for all values of  $\text{Re}$  number below 1.

Moreover, in order to use the same legend for all the presented pressure distributions in the structural units, the normalized pressure drop is defined as:

$$p^*(x,y) = \frac{p(x,y)}{\langle p \rangle^f|_{x=0}} \tag{16}$$

#### 4. NUMERICAL PROCEDURE

The continuity and Navier-Stokes equations (Eqs. 6-8) are solved by using Ansys 12.1. The power law scheme was used for the treatment of the convective term in the momentum equation and SIMPLE scheme is used to treat the pressure-velocity coupling. The residual convergence criterion is set to  $10^{-9}$ . The discretization interval is chosen to be 0.02 mm, resulting in 501x501 of grids for the entire domain. The study is performed for air with density of  $1.205 \text{ kg/m}^3$  and dynamic viscosity of  $18.21 \cdot 10^{-6} \text{ kg/ms}$ . The considered Reynolds numbers are lower than 1. After finding periodic velocity distributions in the structural units, the macroscopic pressure drops and velocities are calculated by using Eqs. (13) and (14). Finally, the permeability is found by using Eq. (15) with computed values of macroscopic pressure gradient and macroscopic velocity. To determine Kozeny constant, Eq. (4) with the obtained permeability values and the pore hydraulic diameters of the porous media are used. Although the dimensional equations are solved in this study, the results and suggested correlation are presented based on dimensionless geometrical parameters (see Table 3) for

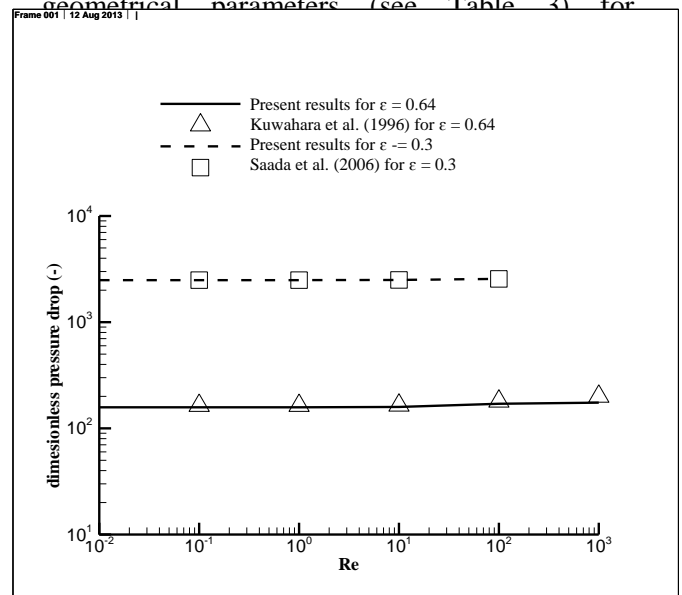


Fig. 2 Comparison of obtained results with those of Kuwahara et al. (1996) and Saada et al. (2006) for variation of dimensionless pressure drop with Reynolds number.

The dimensionless pressure drop values of the present study are compared with the values reported by Kuwahara et al., (1996) (for a square rod porous media with porosity 0.64 and  $10^{-2} < \text{Re} < 10^3$ ) and Saada et al., (2006) (for square rod porous media with porosity 0.3 and  $10^{-2} < \text{Re} < 10^2$ ) as seen in Fig. 2. Additionally, the change of the

dimensionless pressure drop with porosity is compared with the results of Saada et al., (2006) in Fig. 3. The obtained values of the present study and the reported literature values for dimensionless pressure drop are in good agreement with each other.

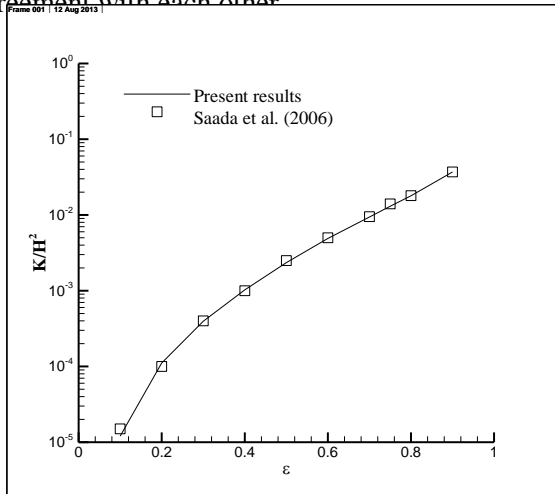


Fig. 3 Comparison of obtained results with those of Saada et al. (2006) for variation of dimensionless permeability with porosity.

## 5. RESULTS AND DISCUSSION

The change of dimensionless pressure drop with Re number for the considered  $\epsilon$  and  $\beta$  values are checked to ensure that the Darcy's Law is valid and the considered cases are in Darcy Region. The dimensionless pressure drop does not vary with Re number for the region of  $Re < 1$  which is Darcian region. The value of dimensionless pressure drop increases with decrease of porosity or increase of pore to throat size ratio. For example, the value of dimensionless pressure drop increases from 1069.4 to 2257.4 by decrease of  $\epsilon$  from 0.9 to 0.7 for  $\beta = 7.46$ . Similarly, the value of dimensionless pressure drop increases from 50.44 to 2257.4 by increase of  $\beta$  from 1.63 to 7.46 for  $\epsilon = 0.7$ .

There are two cases in this study which have the same porosity, hydraulic pore diameter and equivalent particle diameter but different pore to throat size ratios. Geometrical properties of these cases are given in Table 3. The structural units with pore to throat size ratios of 1.63 and 4.44 for the porosity of 0.7 have the same hydraulic and particle diameters. Hence the expected result is the same permeability value for these two structural units. However, the dimensionless pressure drop values for these structural units are approximately ten times different from each other (50.44 for  $\beta = 1.63$  and 583.45 for  $\beta = 4.44$ ). The value of permeability is generally considered a function of porosity in the literature but the

present results show that the permeability does not only depend on the porosity. The effects of pore throat size ratio should also be taken into account in order to find a general relationship for determination of permeability.

In order to understand the change of flow field in the voids between the rods, the streamlines and the normalized pressure distributions in the structural units with  $\beta = 7.46$  but various porosities are shown in Fig. 4. The normalized pressure distributions are presented by colour contours and the legend on the top of the figures is valid for all cases of Fig. 4. The normalized pressures at the inlets are around 1 for all cases. As can be seen from the normalized pressure distributions, the highest pressure drop occurs in the porous medium with  $\epsilon = 0.2$ . The pressure drops through the structural units decrease with increasing porosity. Moreover, the flow patterns vary with the value of porosity and many secondary flows with different shapes in different regions of the structural units may occur. The main flow through the structural unit with  $\epsilon = 0.2$  is straightforward and resembles a channel flow. Many secondary flows occur at the top and bottom gaps between particles. Number of the secondary flows in the top and bottom gaps between the rods decreases with the increase of  $\epsilon$  from 0.2 to 0.4. The flow enters the bottom and top gaps by the increase of the porosity. The areas occupied by the secondary flows also decrease. This entrance of the main flow into the top and bottom gaps is such that the top and bottom secondary flows split to two separate vortices for porosity of 0.8 and 0.9, as seen from Figs. 4g and 4h.

The streamlines and the normalized pressure distributions for different values of pore to throat size ratio are displayed in Fig. 5 when  $\epsilon = 0.75$ . Similar to Fig. 4, the pressure distributions in the structural unit are normalized and plotted by colour contours. The legend on the top of Fig. 5 is valid for all cases of the figure. The values of normalized pressures at the inlets are around 1 for all presented cases. The pressure drop is relatively low for  $\beta = 1.63$ . There are vortices in the top and bottom gaps between the rods. The main flow is straightforward and does not enter to the top and bottom gaps between the rods. The pressure drop increases and the main flow penetrates to the top and bottom gaps by the increase of  $\beta$ . There are almost four vortices in the different regions of the structural unit of porous medium with  $\beta = 4.44$ .

The change of dimensionless pressure gradient with porosity is shown in Fig. 6 for the range of pore to throat size ratios from 1.63 to 7.46. The

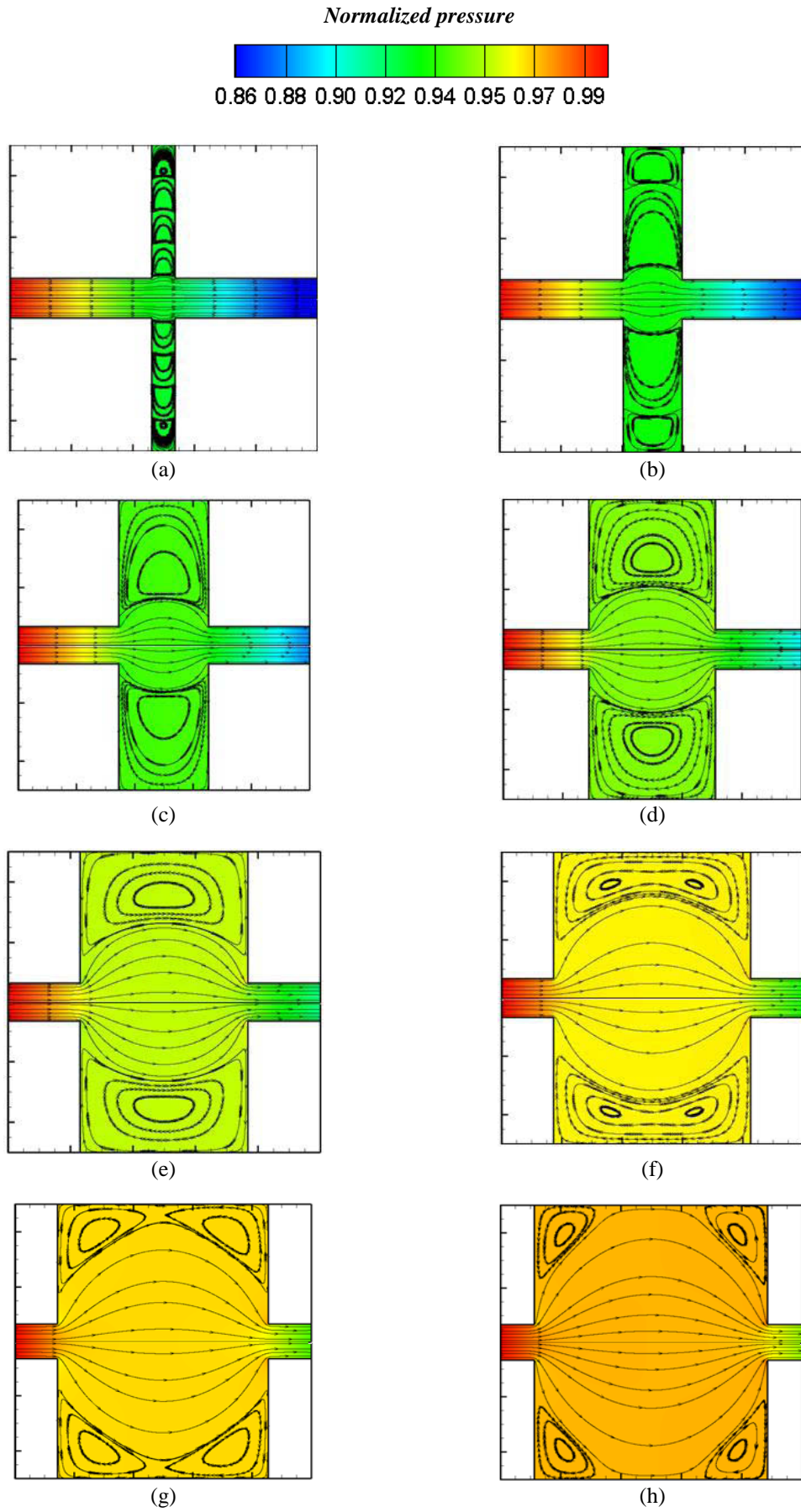


Fig. 4 Streamlines and pressure contours in porous media with different porosities for  $\beta = 7.46$  for porosities of (a) 0.2, (b) 0.3, (c) 0.4, (d) 0.5, (e) 0.6, (f) 0.7, (g) 0.8 and (h) 0.9.

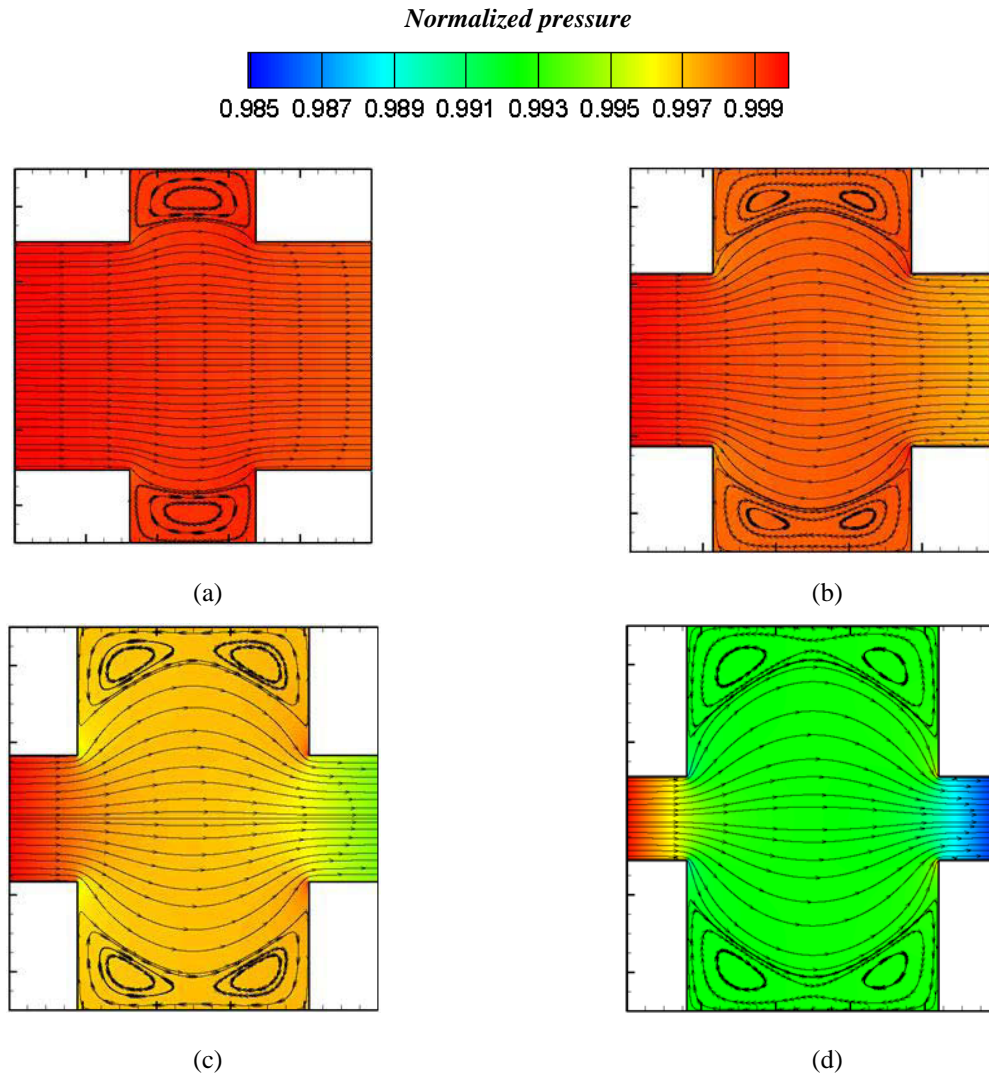


Fig. 5 Streamlines and pressure contours in porous media with different ratios of pore to throat size for  $\epsilon = 0.75$  and for pore to throat size ratios of (a) 1.63, (b) 2.21, (c) 3.04 and (d) 4.44.

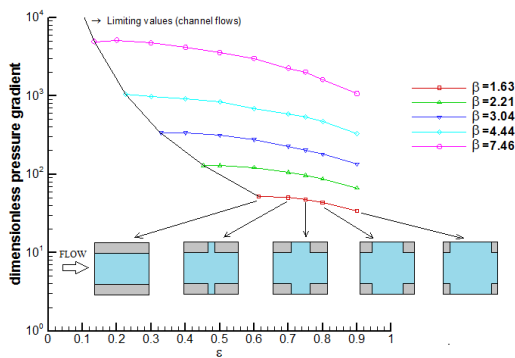


Fig. 6 Change of dimensionless pressure gradient with porosity for porous media with different ratios of pore to throat size.

limiting values represent dimensionless pressure gradients in the straight channel flows with the same throat sizes. The schematics of the structural units for  $\beta = 1.63$  with different porosities are also

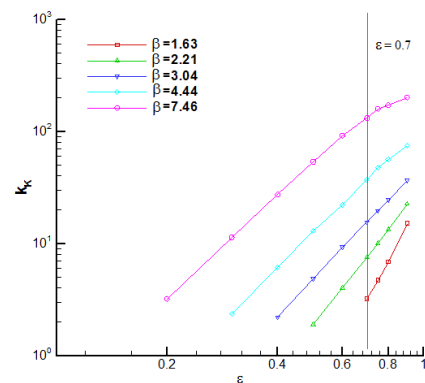


Fig. 7 Variation of Kozeny constant with porosity for different pore to throat size ratios.

shown in Fig. 6. As expected, the dimensionless pressure drop increases with the increase of  $\beta$  while it decreases with the increase of porosity value.

The dimensionless pressure drop is defined based on the structural unit dimension (i.e., H). This value is the same for all studied structural units of the present study. However, in order to find Kozeny constant, Eq. (4) should be used in which the permeability is defined based on the hydraulic diameter. The variation of Kozeny constant with porosity is illustrated in Fig. 7 for the pore to throat size ratios studied in this work. As can be seen from this figure, the value of Kozeny constant depends on both  $\epsilon$  and  $\beta$ . Almost a linear variation of Kozeny constant with porosity is observed for all values of pore to throat size ratio at low porosities (i.e.,  $\epsilon < 0.7$ ). However, the slope of Kozeny constant with  $\epsilon$  is changed for  $\epsilon > 0.7$ .

An attempt is made to obtain a general equation for Kozeny constant based on pore to throat size ratio and porosity. As can be seen from Fig. 7, Kozeny constant generally changes with a power of porosity. Therefore, Eq. (17) may be a proper mathematical relationship for the change of Kozeny constant with porosity for  $0.2 < \epsilon < 0.9$  and  $1.63 < \beta < 7.46$ .

$$k_K = A\epsilon^B \tag{17}$$

where the coefficients A and B are functions of pore to throat size ratio and the following equations are proposed to calculate their values:

$$A = C_0\beta^4 + C_1\beta^3 + C_2\beta^2 + C_3\beta + C_4 \tag{18}$$

$$B = D_0\beta^4 + D_1\beta^3 + D_2\beta^2 + D_3\beta + D_4 \tag{19}$$

Based on the obtained Kozeny constant values, the coefficients of Eqs. (18) and (19) are calculated and given in Table 4 for two different regions separated by the porosity value of 0.7 ( $\epsilon < 0.7$  and  $\epsilon \geq 0.7$ ). The coefficient of determination ( $R^2$ ) values for A and B coefficients are 1 for  $\epsilon < 0.7$  region and 0.9998 and 0.9992 for  $\epsilon \geq 0.7$ , respectively.

Based on Eq. (4), a linear variation exists between the terms of  $16Kk_K/d_h^2$  and  $\epsilon$ . This linear variation with slope of 45 degrees can be seen in Fig. 8 as a solid line. For all cases considered in this study, the values of Kozeny constant, hydraulic diameter and permeability are determined by using Eqs. (17), (5) and (4), then the ratio of  $16Kk_K/d_h^2$  is determined and plotted with respect to  $\epsilon$ . As seen from Fig. 8, the computed results (based on the proposed model) linearly changes with  $\epsilon$  when  $\epsilon < 0.7$ . Although the computed values for  $\epsilon \geq 0.7$  do not fit the solid line as well as for  $\epsilon < 0.7$ , a good agreement can still be observed. This linear relationship between the computed values from the proposed model and  $\epsilon$  exists if only the Kozeny constant is determined as a function of

both porosity and pore to throat size ratio. Hence, the suggested relation for determination of Kozeny constant can gather the effects of both porosity and pore to throat size ratio into a single mathematical relation and provides acceptable results for calculation of permeability for wide ranges of porosity and pore to throat size ratio of porous media. It should be mentioned that the proposed relation is valid only for a porous medium with rectangular rods in a periodic inline arrangement and square structural unit.

Table 4 Empirical coefficients for determination of Kozeny constant.

	For $\epsilon < 0.7$	For $\epsilon \geq 0.7$
$C_0$	-0.6372	0.3496
$C_1$	12.358	-5.6485
$C_2$	-72.413	36.482
$C_3$	199.52	-77.519
$C_4$	-172.44	80.773
$D_0$	0.0079	0.0242
$D_1$	-0.1684	-0.4878
$D_2$	1.33	3.6015
$D_3$	-4.7367	-11.958
$D_4$	9.7242	18.028

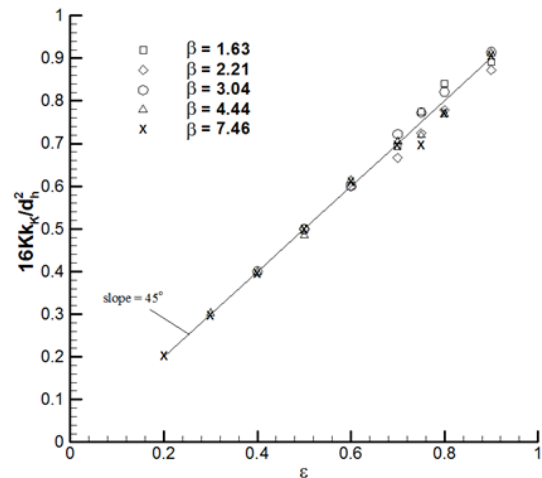


Fig. 8 Comparison of predicted  $16Kk_K/d_h^2$  values by using Eq.s (4), (5) and (17) with Kozeny-Carman permeability equation.

## 6. CONCLUSIONS

The effects of the pore to throat size ratio on the permeability and Kozeny constant in porous media consisting of rectangular rods are investigated, numerically. The continuity and momentum equations are solved for the studied structural units, and the velocity and pressure fields are presented. It is observed that the flow penetrates to the gaps between bars in the flow direction by increasing porosity or pore to throat

size ratio. A detailed literature review is performed and it is found that Kozeny constant was suggested either as a constant value or a function of porosity which is valid for a narrow range of geometrical parameters of a specific porous medium. For two porous media with the same porosity and hydraulic diameter ( $d_h/H = 1.207$ ,  $\varepsilon = 0.7$ ), the values of permeability changes when values of  $\beta$  is different (i.e.,  $\beta = 1.63$  and  $3.04$ ). Hence, Kozeny constant cannot depend only on porosity and the effect of pore to throat size ratio (i.e.  $\beta$ ) should be taken into account to enhance the applicability of Kozeny-Carman equation for wide ranges of the geometrical parameters. Moreover, an equation for Kozeny constant in terms of porosity and pore to throat size ratio is suggested for the studied periodic structure. The proposed equation provides accurate results for the determination of the permeability for porosity range from 0.2 to 0.9 and pore to throat size ratio values from 1.63 to 7.46.

For further studies, the aspect ratio of the structural unit may be changed and the effect of pore to throat size ratio on the permeability for the periodic porous media with different aspect ratios of structural unit can be investigated. Future investigations may be done on the relationship between tortuosity and porosity and pore to throat size ratios to provide further understanding of the effect of pore to throat size ratio on permeability.

## ACKNOWLEDGEMENT

The authors acknowledge the Scientific and Technical Research Council of Turkey, TUBITAK, for 2211 scholarship for Ph.D. students. Furthermore, the authors wish to express their sincere thanks to the reviewers for their valuable comments and suggestions.

## NOMENCLATURE

$A_0$	ratio of fluid-solid interfacial area to the solid volume [1/m]
$A^*$	aspect ratio of bars
$D_x$	dimension of rectangular rod in x-direction [m]
$D_y$	dimension of rectangular rod in y-direction [m]
$d_h$	hydraulic diameter [m]
$d_t$	channel diameter [m]
$H$	dimension of structural unit [m]
$K$	permeability [ $m^2$ ]
$k_K$	Kozeny constant
$p$	pressure [Pa]

$\langle p \rangle^f$	macroscopic pressure in fluid phase [Pa]
$p^*$	normalized pressure
$Re$	Reynolds number ( $=\rho \langle u \rangle H/\mu$ )
$u$	velocity in x-direction [m/s]
$\langle u \rangle$	macroscopic velocity in x-direction [m/s]
$\langle u \rangle^f$	fluid macroscopic velocity [m/s]
$v$	velocity in y-direction [m/s]
$\beta$	pore to throat size ratio ( $=H/(H-D_y)$ )
$\varepsilon$	porosity
$\mu$	dynamic viscosity of fluid [ $kg/m \cdot s$ ]
$\nu$	kinematic viscosity of fluid [ $m^2/s$ ]
$\rho$	fluid density [ $kg/m^3$ ]
$\tau$	tortuosity

## REFERENCES

1. Bechtold G, Ye L (2003). Influence of fibre distribution on the transverse flow permeability in fibre bundles. *Composites Science and Technology* 63:2069-2079.
  2. Carman PC (1937). Fluid flow through granular beds. *Chemical Engineering Research & Design: Transactions of the Institution of Chemical Engineers Part A*. 15:415-421.
  3. Chen X, Papathanasiou TD (2006). On the variability of the Kozeny constant for saturated flow across unidirectional disordered fiber arrays. *Composites Part A* 37:836-846.
  4. Darcy H (1856). *Les Fontaines Publiques de la ville de Dijon*, Dalmont, Paris.
  5. Davies L, Dollimore D (1980). Theoretical and experimental values for the parameter  $k$  of the Kozeny–Carman equation as applied to sedimenting suspensions. *Journal of Physics D: Applied Physics* 13:2013–2020.
  6. Drummond JE, Tahir MI (1984). Laminar viscous flow through regular arrays of parallel solid cylinders. *International Journal of Multiphase Flow* 10:515-540.
  7. Eidsath A, Carbonell RG, Whitaker S, Herrmann LR (1983). Dispersion in pulsed systems-III: Comparison between theory and experiments for packed beds. *Chemical Engineering Science* 38:1803-1816.
  8. Ergun S (1952). Fluid flow through packed columns. *Chemical Engineering Progress* 48:89-94.
- Gamrat G, Favre-Marinet M, Le Person S (2008). Numerical study of heat transfer over banks of rods in small Reynolds number cross-flow. *International Journal of Heat and Mass Transfer* 51:853-864.

9. Happel J, Brenner H (1986). *Low Reynolds Number Hydrodynamics*. Martinus Nijhoff Publishers. Dordrecht.
- Heijs AWJ, Lowe CP (1995). Numerical evaluation of the permeability and the Kozeny constant for two types of porous media. *Physical Review E* 51:4346-4352.
10. Kalita JC, Dass AK (2011). Higher order compact simulation of double-diffusive natural convection in a vertical porous annulus. *Engineering Applications of Computational Fluid Mechanics* 5:357-371.
11. Karimian SAM, Straatman AG (2008). CFD study of the hydraulic and thermal behavior of spherical-void-phase porous materials. *International Journal of Heat and Fluid Flow* 29:292-305.
12. Kaviany M (1995). *Principle of Heat Transfer in Porous Media*. Springer. 2<sup>nd</sup> edition. New York.
13. Koponen A, Kataja M, Timonen J (1997). Permeability and effective porosity of porous media. *Physical Review E* 56:3319-3325.
14. Kozeny J (1927). Ueber kapillare Leitung des Wassers im Boden. *Sitzungsber Akad. Wiss.* 136: 271-306.
15. Kuwahara F, Nakayama A, Koyama H (1996). A numerical study of thermal dispersion in porous media. *Journal of Heat Transfer* 118:756-761.
16. Kyan CP, Wasan DT, Kintner RC (1970). Flow of single-phase fluids through fibrous beds. *Industrial and Engineering Chemistry Fundamentals* 9:596-603.
17. Li J, Gu Y (2005). Coalescence of oil-in-water emulsions in fibrous and granular beds. *Separation and Purification Technology* 42:1-13.
18. Liu HL, Hwang WR (2012). Permeability prediction of fibrous porous media with complex 3D architectures. *Composites Part A* 43:2030-2038.
19. Mathavan GN, Viraraghavan T (1992). Coalescence/filtration of an oil-in-water emulsion in a peat bed. *Water Research* 26:91-98.
20. Nakayama A. (1995). *PC-Aided Numerical Heat Transfer and Convective Flow*. CRC Press.
21. Nakayama A, Kuwahara F, Sano Y (2007). Concept of equivalent diameter for heat and fluid flow in porous media. *AIChE Journal* 53:732-736.
22. Nakayama A, Kuwahara F, Umemoto T, Hayashi T (2002). Heat and fluid flow within an anisotropic porous medium. *Journal of Heat Transfer* 124:746-753.
23. Pacella HE, Eash HJ, Frankowski BJ, Federspiel WJ (2011). Darcy permeability of hollow fiber bundles used in blood oxygenation devices. *Journal of Membrane Science* 382:238-242.
24. Plessis JP, Woudberg S (2008). Pore-scale derivation of the Ergun equation to enhance its adaptability and generalization. *Chemical Engineering Science* 63:2576-2586.
25. Reddy KS, Satyanarayana, GV (2008). Numerical study of porous finned receiver for solar parabolic trough concentrator. *Engineering Applications of Computational Fluid Mechanics* 2: 172-184.
26. Saada MA, Chikh S, Campo A (2006). Analysis of hydrodynamic and thermal dispersion in porous media by means of a local approach. *Heat and Mass Transfer* 42:995-1006.
27. Singh M, Mohanty KK (2000). Permeability of spatially correlated porous media. *Chemical Engineering Science* 55:5393-5403.
28. Teruel FE, Rizwan-uddin (2009). Characterization of a porous medium employing numerical tools: Permeability and pressure-drop from Darcy to turbulence. *International Journal of Heat and Mass Transfer* 52:5878-5888.
29. Vidal D, Ridgway C, Pianet G, Schoelkopf J, Roy R, Bertrand F (2009). Effect of particle size distribution and packing compression on fluid permeability as predicted by lattice-Boltzmann simulations. *Computers and Chemical Engineering* 3: 256-266.
30. Xu P, Yu B (2008). Developing a new form of permeability and Kozeny-Carman constant for homogeneous porous media by means of fractal geometry. *Advances in Water Resources* 31:74-81.